A Novel Multi-purpose MIP for SPE-HPLC and QCM Detection of Carbaryl Residues in Foods

Chang Liu[1] · Yichuan Cao[1] · Tian Zhao[1] · Xiaohui Wang[1] · Guozhen Fang[1] · Shuo Wang[1,2]

Abstract

In this work, two detection methods of solid-phase extraction–high-performance liquid chromatography (SPE-HPLC) and quartz crystal microbalance (QCM) were established, based on a surface molecularly imprinted polymer material (MIP). The material can be used as a selective solid-phase extraction filler and as a coating for sensitive quartz crystal microbalances by virtue of the polyhydroxy structure of grafted silicon spheres together with the network structure from cross-linked polymerization. The adsorption properties of the prepared MIP were analysed by dynamic and static adsorption tests, and the experimental conditions for SPE-HPLC and QCM analysis were optimized. Under the optimal conditions, the linear range of MIP-SPE-HPLC for the detection of carbaryl was 0.5–60 $\mu g\,L^{-1}$ ($R^2 = 0.99913$), and the detection limit was 0.0573 $\mu g\,L^{-1}$. The proposed QCM sensor displayed a linear relationship between the frequency shift and the concentration of carbaryl ranging from 5 to 80 $\mu g\,L^{-1}$ with a low detection limit of 0.6845 $\mu g\,L^{-1}$ (signal-to-noise ratio, S/N = 3). Through a series of experiments, it was shown that the prepared MIP has good adsorption and selectivity for carbaryl, and the MIP-based HPLC and QCM sensor can be applied to the detection of actual food samples.

Introduction

Carbaryl, a carbamate pesticide that was discovered in 1956 by the USA, has been widely used as an insecticide in agriculture due to its low persistence, broad-spectrum activity, high insecticidal activity, and stability at room temperature and sunlight. However, widespread and improper use of this pesticide is detrimental to the environment and poses health risks. Residual carbaryl can enter into the human body through the respiratory tract, skin and mucous membranes, or digestive tract due to the bio-accumulation, and can act as an acetylcholinesterase inhibitor that may damage the nervous systems, muscles, liver, pancreas, and brain (Karami-Mohajeri and Abdollahi 2011). Therefore, the pesticide residues are serious life-threatening contaminants that have raised serious public concerns regarding food safety and human health, as well as the rapid determination and reliable quantification of carbaryl. Various countries have certain requirements for the carbaryl residue limits in foods. For example, the tolerances for carbaryl residues in apple are 15 mg kg⁻¹ in the USA (U.S. GPO, 2020), and the maximum residue levels of carbaryl in round lettuce are 1 mg kg⁻¹ in China (GB2763-2019, China, 2019), 5 mg kg⁻¹ for pear in Japan (the Japan Food Chemical Research Foundation 2019), and 0.01 mg kg⁻¹ for apple in the EU (European Commission 2014).

Many methods, such as high-performance liquid chromatography (HPLC) (Hargreaves and Melksham 1983), liquid chromatography/gas chromatography/mass spectrometry (HPLC-MS/GC-MS) (Hernández et al. 2013; Petropoulou et al. 2006), and enzyme-linked immunosorbent assay (ELISA) (Sun et al. 2010), have been used to measure carbaryl residues. These common methods have the advantages of accurate detection results and low detection limits. However, the pre-processing is cumbersome, the detection time is long, and the use conditions are strict. New methods for detecting analytes selectively, quickly, or under mild conditions have

✉ Guozhen Fang
fangguozhen@tust.edu.cn

✉ Shuo Wang
s.wang@tust.edu.cn

1 State Key Laboratory of Food Nutrition and Safety, Tianjin University of Science and Technology, Tianjin 300457, China

2 Tianjin Key Laboratory of Food Science and Health, School of Medicine, Nankai University, Tianjin 300071, China

emerged, for instance, solid-phase microextraction coupled with high-performance liquid chromatography (SPME-HPLC), rapid colorimetric detection (Lee et al. 2018), nano-carbon black-based screen-printed sensors (CB-SPE) (Pelle et al. 2018), Raman spectroscopy (SERS) (Alsammarraie and Lin 2017), electrochemistry (Rahmani et al. 2018) and quartz crystal microbalance (Karousos et al. 2002), some new methods based on ELISA (Zhang et al. 2017), and show us new ideas and progress. These detection methods have different advantages and disadvantages, respectively. The accurate detection results, high efficiency, and sensitivity may be supported by time-consuming operations, complicated sample pretreatment, expensive machines, highly trained personnel, or poor repeatability. Therefore, motivated by these past advances, we aim to establish a new way to detect pesticide residues more easily, accurately, quickly, and even cost-effectively.

The molecular imprinting technique (MIT) is a synthetic method of polymer materials exhibiting a specific binding ability to a certain molecule. Currently, MIT has been widely used in various aspects of food safety testing. Its superb recognition and adsorption capability and desirable stability provide great convenience for detection. Furthermore, the quartz crystal microbalance (QCM) is a mass-sensitive sensor capable of measuring mass changes in the nanogram range (Bruckenstein and Shay 1985). The increased mass loaded onto the surface of sensor chips results in a decrease in the frequency response of the sensor. Therefore, the combination of an outstandingly selective molecularly imprinted polymer (MIP) with the ultra-sensitive quartz crystal microbalance will result in a superior chemical sensor. In recent years, there have been many reports on the detection methods of quartz crystal microbalance sensors based on molecular imprinting technology, such as the detection of caffeic acid in plant materials (Gültekin et al. 2014), albumin in serum (Lin et al., 2005), amoxicillin antibiotics in aqueous samples (Ayankojo et al. 2018), cholic acid levels in body fluids (Gültekin et al. 2014), and *Bacillus cereus* in distilled water (Spieker and Lieberzeit 2016). However, most of the QCM methods used to detect carbaryl are immunosensors or enzyme sensors based on specific antigen-antibody recognition (Carmen et al. 2015; Cervera-Chiner et al. 2018) or enzyme cascades (Karousos et al. 2002). Although these methods are specific, sensitive, and inexpensive, the enzyme is also sensitive to external influences (temperature and pressure), and new quartz chips and analytical instruments are needed (Gaudin 2017) and have certain requirements for storage conditions. Therefore, we tried to synthesize a molecularly imprinted polymer with improved performance and combined it with QCM to establish simple, easy-to-use, low-cost methods that do not need trained professionals for the detection of carbaryl residues in food.

In this work, the MIP was synthesized on the surface of the grafted silicon spheres on which had a polyhydroxy network structure (Husseman et al. 1999). The MIP obtained by this means had enlarged specific surface area and held more methacrylic acid, assisting the formation of molecularly imprinted polymers and providing more imprinted recognition sites. By applying the MIP to the solid-phase extraction before HPLC analysis, the target molecules could be adsorbed with high efficiency and high selectivity. In combination with QCM, a highly sensitive and highly selective sensor for the determination of carbaryl could be established. These two detection methods were demonstrated to be feasible and effective by verifying the measurements in the actual samples. The preparation of the MIPs, as well as the application and optimization of the two detection methods are described and discussed below. The preparation and detection processes of the MIP, SPE-HPLC, and MIP-QCM sensors are shown in Fig. 1.
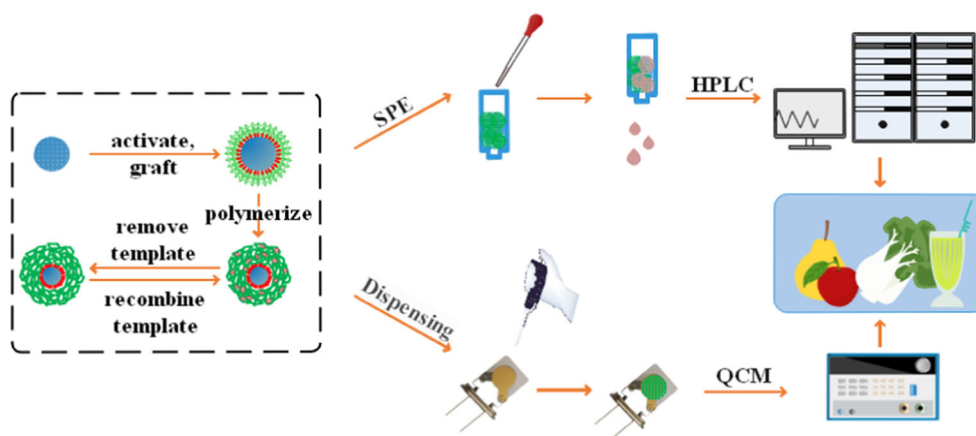
Experimental

Reagents and Materials

Carbaryl (99.9%), metolcarb (99.7%), propoxur (99.9%), and isoprocarb (97.6%) were purchased from Dr. Ehrenstorfer GmbH (Germany), and the chemical structural formulas are shown in Fig. 2. Methacrylic acid (MAA, 99%), azodiisobutyronitrile (AIBN, 98%), ethylene glycol dimethacrylate (EGDMA, 97%), and methanesulfonic acid (99%) were achieved from TCI Shanghai Chemical Industry Development Co., Ltd. (Shanghai, China). Chloroform, acetonitrile (ACN), methanol (MeOH), glacial acetic acid (HAC), ethyl alcohol (EtOH), and dichloromethane (DCM) were obtained from Tianjin Chemical Reagent Plant (Tianjin, China). Polyvinyl chloride (PVC) and γ-methacryloxypropyltrimethoxysilane (γ-MPS, 98%) were supplied by Sigma-Aldrich (St. Louis, MO, USA) and Ourchem Sinopharm Chemical Reagent Co., Ltd. (Shanghai, China), respectively. All of the reagents were at least analytical grade. Doubly deionized water (DDW, 18.2 MΩ cm^{-1}) obtained from a Milli-Q water purification system was used throughout the experiment. The food samples, i.e. apple, pear, and round lettuce, were purchased from a local supermarket. Silica sphere (5 μm) were purchased from Borui Bonded Chromatography Technology Co., Ltd. (Tianjin, China).

Apparatus and Instruments

The measurement of frequency shift (*f*, Hz) was carried out by the QCM instrument (QCM-922, Princeton Applied Research, Princeton, NJ, USA) equipped with a 9 MHz AT-

Fig. 1 The preparation and detection process of MIP, SPE-HPLC, and MIP-QCM sensor

cut quartz crystal (Seiko EG&G) coated with Au electrode (AuE, 0.196 cm^2) on both sides. In the experiments, the quartz crystal was installed into the Teflon holder (well-type, QA-CL3, Seiko EG&G) to ensure that only one side of the quartz crystal contacted the solution to be tested. Scanning electron microscopy (SEM, SU1510, HITACHI, Tokyo, Japan) was used to observe the surface morphological characteristics of the MIP. The adsorption effect of MIP and NIP on the target was measured and evaluated by an ultraviolet spectrophotometer (EVO300PC, Thermo Fisher Scientific Inc., USA). HPLC (LC-20AB, Shimadzu, Japan) was utilized to validate the results obtained from the MIP-QCM sensor. HPLC was utilized to determine the content of the target enriched by MIP-SPE and to verify the results of QCM measurement. HPLC analysis was performed using methanol/water (55:45,

v/v) as the mobile phase with a flow rate of 0.8 mL min^{-1} at 30 °C through an analytical octadecylsilyl (ODS) column (4.6 mm × 150 mm, 5 μm particle size, Thermo). The injection volume for each test is 20 μL and the detection wavelength was 222 nm.

Preparation of the MIP

First, silica spheres (10 g) were activated by refluxing with methanesulfonic acid (75 mL, 33%) under electromagnetic stirring for 10 h; afterwards, they were rinsed repeatedly with water until the solution was neutral, and then vacuum-dried at 70 °C for 10 h. Next, 6 g of activated silicon spheres were dispersed in an ethanol-water solution (v:v = 1:1, 400 mL) containing 10 mL of γ-MPS for 24 h at 50 °C. The silicon spheres were filtered with absolute ethanol and vacuum-dried for 10 h.

Then, 2 g of the silicon spheres processed by the above method and 0.200 g (1.0 mmol) of carbaryl were added into a mixture of 30 mL of ACN and 20 mL of chloroform in a round-bottomed flask at room temperature. The mixture was stirred at 60 °C for 1 h after adding the functional monomer (MAA, 0.340 mL, 4.0 mmol). Stirring was continued for 30 min after the cross-linker (EGDMA, 3.760 mL, 20.0 mmol) was added. Then, the initiator (AIBN, 20 mg) was added to the mixture. The mixed solution was sonicated for 5 min, followed by nitrogen purging for 10 min to remove oxygen from the liquid. The round bottom flask containing the mixed solution was then placed in a water bath at 60 °C for 10 h to allow polymerization to be initiated in the mixture by heat. After polymerization, the polymer was rinsed with acetonitrile and dried in a vacuum for 12 h at 60 °C. Next, 300 mL of methanol/acetic acid (9: 1, v/v) were used to separate the target from the polymer by Soxhlet extraction until no target was detected in the eluent by UV spectrometry at 222 nm. Finally, the MIP was obtained. As a control, non-imprinted polymers were obtained under the same conditions, except that no template molecules were added during the synthesis.
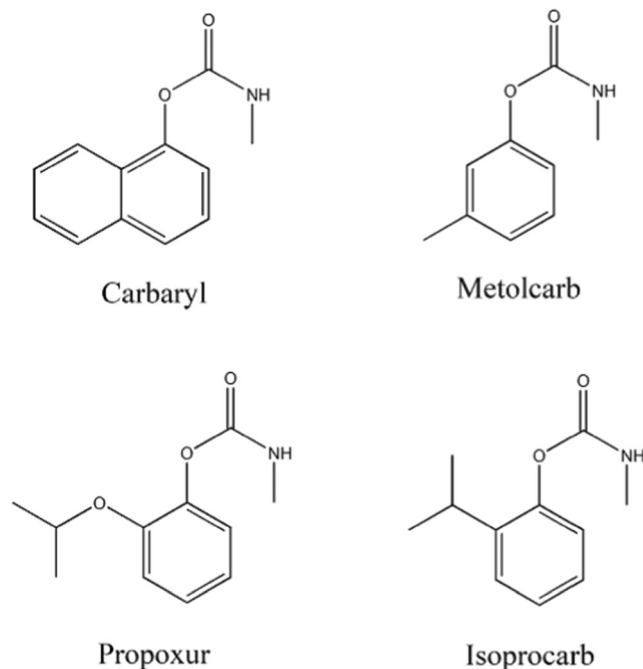
Fig. 2 Chemical structural formulas of carbaryl, metolcarb, propoxur, and isoprocarb

Adsorption Measurements of MIP

First, 20.0 mg of MIP or NIP was added into 15-mL polypropylene centrifuge tubes, which contained 10.0 mL of a carbaryl-methanol solution at different concentrations (10, 20, 30, 40, 50, 60, 80, 100, and 120 mg L^{-1}). Then, after the tubes were shaken and adsorption was allowed to occur at room temperature for 2 h, they were centrifuged at 10,000 rpm for 15 min. The concentration of unadsorbed carnaryl remaining in the solution was determined by its UV absorbance at 222 nm. The adsorption capacity (Q, mg g^{-1}) of the MIP was calculated by Eq. (1) as follows:

$$Q = \left(C_i - C_f\right) \times V/W \qquad (1)$$

where C_i and C_f are the initial and final concentrations of the target in the solution, respectively (mg L^{-1}), V is the volume of the solution (L), and W is the amount of polymer (g).

Establishment of the SPE-HPLC Detection Method

Preparation of SPE Column

The SPE column was prepared as follows: a polypropylene gasket, 60 mg of the weighed MIP material, and another piece of polypropylene gasket were added sequentially into a 3 mL empty SPE column in turn, and they were carefully pressed into the bottom with a glass rod carefully to avoid the column being clogged due to too much filling. The SPE column was activated with 3 mL of methanol and 3 mL of deionized water, and then enriched with 50.0 mL of the standard aqueous solution of carbaryl. The target was enriched on the MIP-SPE column, while the unadsorbed portion flowed out with the eluent. The MIP-SPE column was eluted with methanol and the eluate was collected. Next, the eluate was dried with nitrogen, reconstituted with 1.0 mL of chromatographic grade methanol, filtered through a 0.45 μm filter, and chromatographed.

The experimental conditions of the non-imprinted cartridge (NIP-SPE column) were the same as those of the MIP-SPE column. To compare the selective enrichment effect of the prepared MIP-SPE column, a comparative experiment was carried out using a C18-SPE enriched column. The recovery rates were calculated to evaluate the selectivity and adsorption capacity of the prepared SPE columns, and three parallel experiments were performed.

Optimization of Solid-Phase Extraction Conditions

To investigate the effect of the pH value of the sample solution and the loading flow rate on the solid-phase extraction, the carbaryl standard solution (50 mL, 1 mg L^{-1}, DDW) was tested at different pH values (pH 5.5, 6, 6.5, 7, 7.5, 8, 8.5)

and different flow rates (0.5 mL min^{-1}, 1 mL min^{-1}, 1.5 mL min^{-1}, 2 mL min^{-1}, 2.5 mL min^{-1}, 3 mL min^{-1}).

Optimization of the elution conditions was a critical step in molecularly imprinted solid-phase extraction to achieve satisfactory recovery. First, 12 mL of MeOH, EtOH, ACN, and DDW were selected to elute the solid-phase extraction column after enrichment to compare the elution effect. Then, the SPE column was eluted with 12 mL of the eluent with different durations to select the optimum flow rate. Next, the results of different volume eluent volumes (4 mL, 5 mL, 6 mL, 7 mL, 8 mL, 9 mL, 10 mL, 11 mL, 12 mL) on the elution effect were investigated to avoid wasting resources by using too much eluent. Finally, different elution rates (0.5 mL min^{-1}, 1 mL min^{-1}, 1.5 mL min^{-1}, 2 mL min^{-1}, 2.5 mL min^{-1}, 3 mL min^{-1}, 4 mL min^{-1}, 5 mL min^{-1}) were also tested.

The eluate was dried with nitrogen, and the residue was dissolved in 1 mL MeOH/DDW (55:45, v/v) solution and filtered through a 0.22-μm filter for subsequent HPLC.

Research on the MIP-SPE Column Recycling Performance

The MIP-SPE columns were repeatedly loaded and eluted 5 times under the same conditions, and the eluate obtained each time was analysed by HPLC. The experiment was performed in parallel three times. The recovery rate was calculated to evaluate the recyclability of the MIP-SPE column.

Establishment of the MIP-QCM Detection Method

Preparation of MIP-Coated Quartz Crystal Electrode

An electrode was ultrasonically cleaned in ethanol, dried with nitrogen, and cleaned by freshly prepared piranha solution (30% H_2O_2:98% H_2SO_4, 1:3, v/v) for 5 min. After rinsing thoroughly with water and EtOH, the electrode was dried again with ultra-pure nitrogen. MIP or NIP (8.0 mg) was dispersed in 2 mL PVC-DCM (1.0 mg mL^{-1}). After vortexing for 2 min and sonicating for 5 min, a homogeneous solution was obtained. Then, 5 μL of the mixed solution was carefully dropped on the surface of the quartz crystal each time. The dried modified electrode was stored in a vacuum chamber for later use.

Measurement of the MIP-QCM Sensor

The response of the QCM sensor towards the analyte was evaluated by submerging the quartz crystal resonator assembled in a Teflon retainer into 50 mL of a MeOH solution containing different concentrations of the target with magnetic stirring. First, the initial frequency denoted as f_0 was a stable frequency measured by the sensor in a blank solution (a frequency change less than 1.0 Hz could be regarded as a stable sensor frequency). A small amount of the appropriate high

concentration analyte solution was dropped into the detection cell in portions with a micropipette to achieve the desired concentration of the target solution. When the frequency response value (f_i, Hz) was stable again, a frequency change caused by analyte binding was obtained and recorded. The modified quartz crystal was rinsed with a MeOH/1.0 mol L^{-1} HCl solution (9:1, v/v) and DDW repeatedly until the frequency recovered to f_0 and then was dried with nitrogen for the next measurement. Triplicate analysis was performed and the average of three experiments was used for calculation and analysis. Then, the mass of carbaryl adsorbed by the material on the quartz crystal surface could be calculated by the Sauerbrey equation:

$$\Delta f = -2.26 \times 10^{-6} \Delta m f_0^2 / A$$

where f_0 is the original frequency (Hz), Δm is the mass change (g), A is the surface area of the electrode (cm^2), and Δf is the difference between f_0 and f_i.

For comparison and elimination of interference, the NIP-QCM sensor and PVC-coated sensor were also tested using the same procedure.

Sample Preparation

Prior to the spike and recovery studies, three different sample matrices (apple juice, pear, and lettuce) were determined to be free of carbaryl by HPLC.

Samples (5.00 ± 0.01 g or 5.00 ± 0.01 mL) in 50 mL polypropylene centrifuge tubes were spiked with carbaryl at three levels respectively (50, 100, and 200 µg kg^{-1} or µg L^{-1}) and stored overnight in the dark. Next, 5.0 mL of acetone and 1.0 g of sodium chloride were added into the tubes, which were shaken vigorously for 5 min. After adding 5.0 mL of DCM and 1.0 g of anhydrous Na_2SO_4, the tubes were shaken again for 5 min. Then, the mixture was centrifuged at 6000 rpm for 10 min, and the supernatant was transferred to another centrifuge tube. The residue was treated as described above and the collected supernatants were combined. The supernatant was dried with high-purity nitrogen at 40 °C and then reconstituted with methanol (2 mL).

The sample extracts obtained above were loaded onto an activated C18 solid-phase extraction column (C18-SPE, 60 mg, 3 mL, Bonna-Agela Technologies) and MIP-SPE at a flow rate of 1 mL min^{-1} for purification. The eluent of acetone and DCM (1:1, v/v) was collected, blown dry with nitrogen flow at 40 °C, and then redissolved in 1 mL of MeOH. The reconstituted liquid was filtered with a 0.22 µm nylon filter for HPLC analysis or transferred to a 50 mL volumetric flask and brought to volume with methanol for QCM analysis.

The test results of carbaryl detected by the developed MIP-QCM sensor were verified by the HPLC an ultraviolet detector.

Results and Discussion

Synthesis of the Carbaryl Molecularly Imprinted Material

As the identification and adsorption element of this detection method, the MIP should be synthesized according to a clear reaction route. First, the activation of the silicon spheres by methanesulfonic acid exposed a large amount of hydroxyl groups on their surface. The activated silicon spheres were then modified with γ-MPS and grafted with MAA. The molecularly imprinted polymer was subsequently synthesized on the surface of the silica sphere by precipitation polymerization. During the prepolymerization process, hydrogen bonds were formed between the carboxyl group of MAA and the imino group and carbonyl groups of carbaryl. Then, the carbaryl was encapsulated in the cross-linked network by the effect of a cross-linking agent. When the template molecule carbaryl was washed away, a large number of holes matching the template molecules were left in the thin polymer layer on the surface of the silicon sphere forming a carbaryl molecularly imprinted material.

FT-IR and Morphological Characterization

The FT-IR spectra of the MIP before and after template elution are shown in Fig. 3. Compared with the MIP combined with carbaryl, the MIP after elution did not exhibit the vibrations of the aromatic ring skeleton at 1620 cm^{-1}, 1602 cm^{-1}, 1566 cm^{-1}, and 1490 cm^{-1}, the stretching vibrations of –CH– in the aromatic ring at 3095 cm^{-1}, 3068 cm^{-1}, and 3035 cm^{-1}, or the diffuse band of NH^{2+} at 2559 cm^{-1}. This result shows that MIP-carbaryl was successfully synthesized.
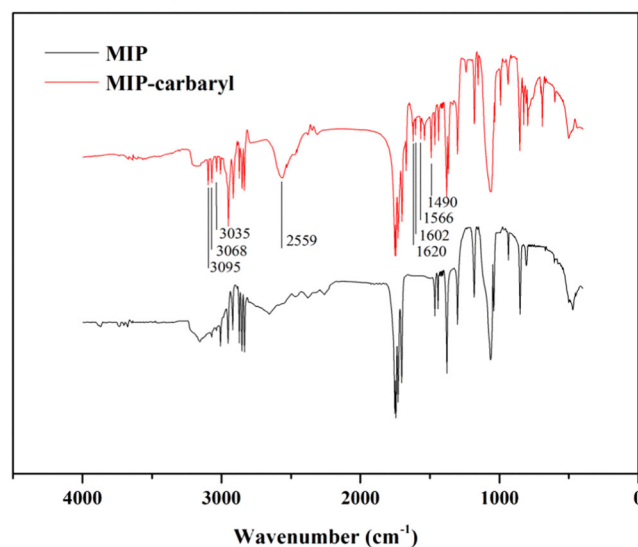

Fig. 3 FT-IR spectrums of MIP before and after template extraction

The morphology of the MIP with silicon microspheres as the support material is shown by SEM in Fig. 4. Due to the thickness of the spheres, the edge of the sphere was scanned. The MIP layer was plump, loose, and multi-porous, which was beneficial to the binding of the target to the specific site of MIP.

Adsorption Study of MIP-Carbaryl

Different adsorption solvents could affect the adsorption capacity of MIP to the target. To select a suitable adsorption solvent, the adsorption capacity of the MIP to the target molecule in different solvents (MeOH, EtOH, ACN, and DDW) was calculated and compared. As illustrated in Fig. 5a, when using MeOH as the adsorption medium, the adsorption capacity of MIP was significantly higher than that when using DDW, EtOH, or ACN. However, in DDW, the adsorption capacity of NIP was also high, indicating that nonspecific adsorption was superior to specific adsorption in DDW, which may be because the target molecules were not readily soluble in water. Instead, there was a threefold gap between the adsorption capacity of the MIP and NIP in MeOH. Thus, MeOH was used as the adsorption solvent in the subsequent experiments.

The adsorption capability (Q, mg g^{-1}) of the prepared MIP and NIP in different concentrations of a carbaryl-methanol solution was determined in parallel three times. The adsorption isotherm curves are shown in Fig. 5b. The adsorption amount of MIP and NIP also increased with the increasing initial concentration of carbaryl. However, at the same initial concentration, the adsorption capacity of the MIP was significantly higher than that of the NIP. At the initial concentration of 120 mg L^{-1}, the adsorption capacities of the MIP and NIP were 5.72 mg g^{-1} and 2.52 mg g^{-1}, respectively.

Scatchard analysis is shown in Fig. 5c. Within the concentration range of 5–80 mg/L, the MIP had a linear relationship between Q/c and Q, which indicated that flawless imprinting sites were formed in the MIP. There was

no good linearity between the Q/c and Q of the NIP, indicating that no uniformly specific imprinting sites were formed in the NIP.

Then, the selectivity of the MIP was investigated, with metolcarb, propoxur, and isoprocarb as interfering substances. The adsorption results of the MIP with the four substances are shown in Fig. 5d. There were different degrees of adsorption effects with the four analytes, which may be caused by the structural similarity of the analytes and the multi-hole structure of the adsorbent material. It was obvious that the MIP had the best adsorption effect on the target carbaryl, which indicated that the MIP material forms excellent imprinted holes according to the shape, structure, and size of the target so that the target can be effectively recognized and captured. Tailored cavities were not formed in the NIP, which results in the adsorption of the NIP being purposeless, nonspecific, indistinguishable, and much lower than that of MIP to the target, showing no significant advantage compared with the adsorption of the structural analogues.

Condition Optimization and Establishment of the SPE-HPLC Detection Method

Optimization of Loading Conditions

The pH value of the carbaryl standard solution was adjusted with dilute hydrochloric acid and dilute sodium hydroxide solution to detect the effect of different pH values on the recovery rate of the solid-phase extraction column. The result in Fig. 6a shows that the recovery of solid-phase extraction was lower in the acidic environment and increased gradually with increasing pH in the range of pH 5.5 to 7. When the pH value was increased from 7.5, the recovery rate showed a downward trend. Therefore, the best absorption effect of the solid-phase extraction column was achieved under neutral alkaline
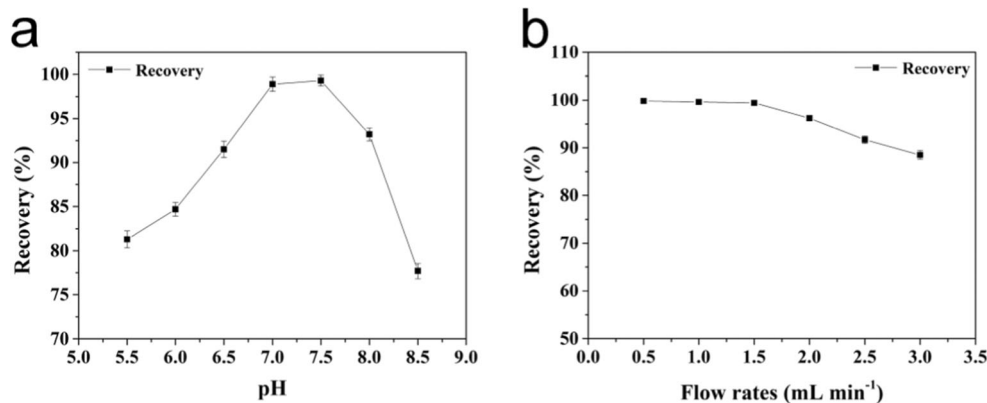

Fig. 4 SEM images of MIP
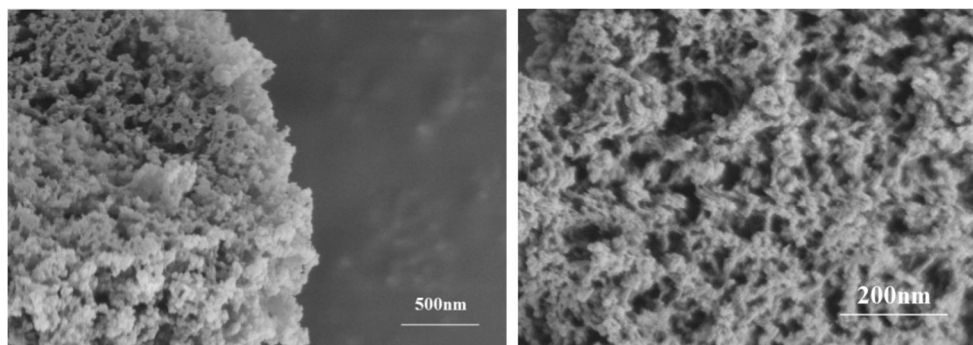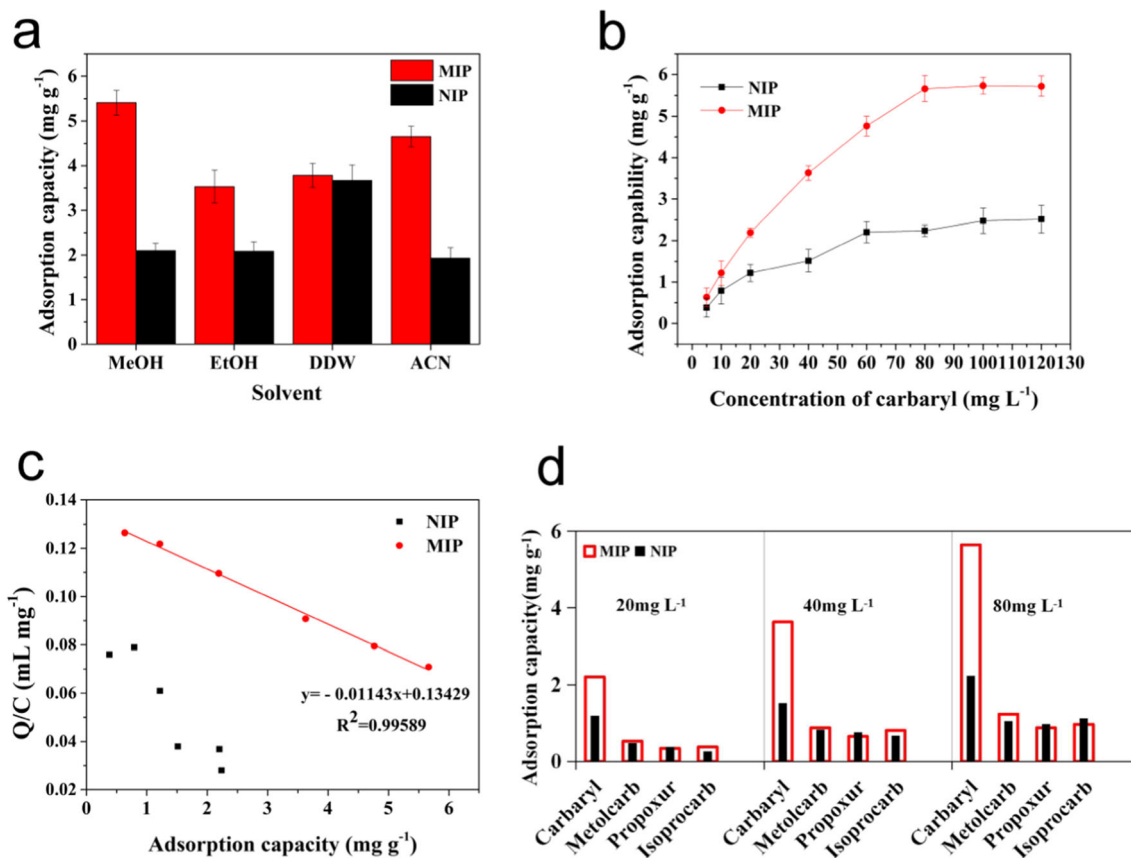
Fig.5 **a** The effect of different solvents on adsorption properties. **b** Binding isotherm of MIP and NIP for carbaryl in methanol. **c** Scatchard analysis of MIP and NIP. **d** Adsorption properties of NIP and MIP for different concentrations of carbaryl, metolcarb, propoxur, and isoprocarb

conditions, and the pH of the sample solution was kept from 7 to 7.5 during the experiment.

The loading rate affects the adsorption of MIP on carbaryl. Excessive flow rates could cause the target to not be completely adsorbed by the MIP, resulting in a decrease in recovery. Slower flow rates reduce the efficiency. Therefore, according to Fig. 6b, a flow rate of 1 mL min^{-1} could be used.

Optimization of the Elution Conditions for SPE

After loading under the same conditions, the MIP-SPE columns were eluted with different elution solutions, different eluent volumes, or different elution rates, and the recovery rates were calculated separately. The average of the three sets of recoveries for each test is plotted in Fig. 7 a, b, and c.
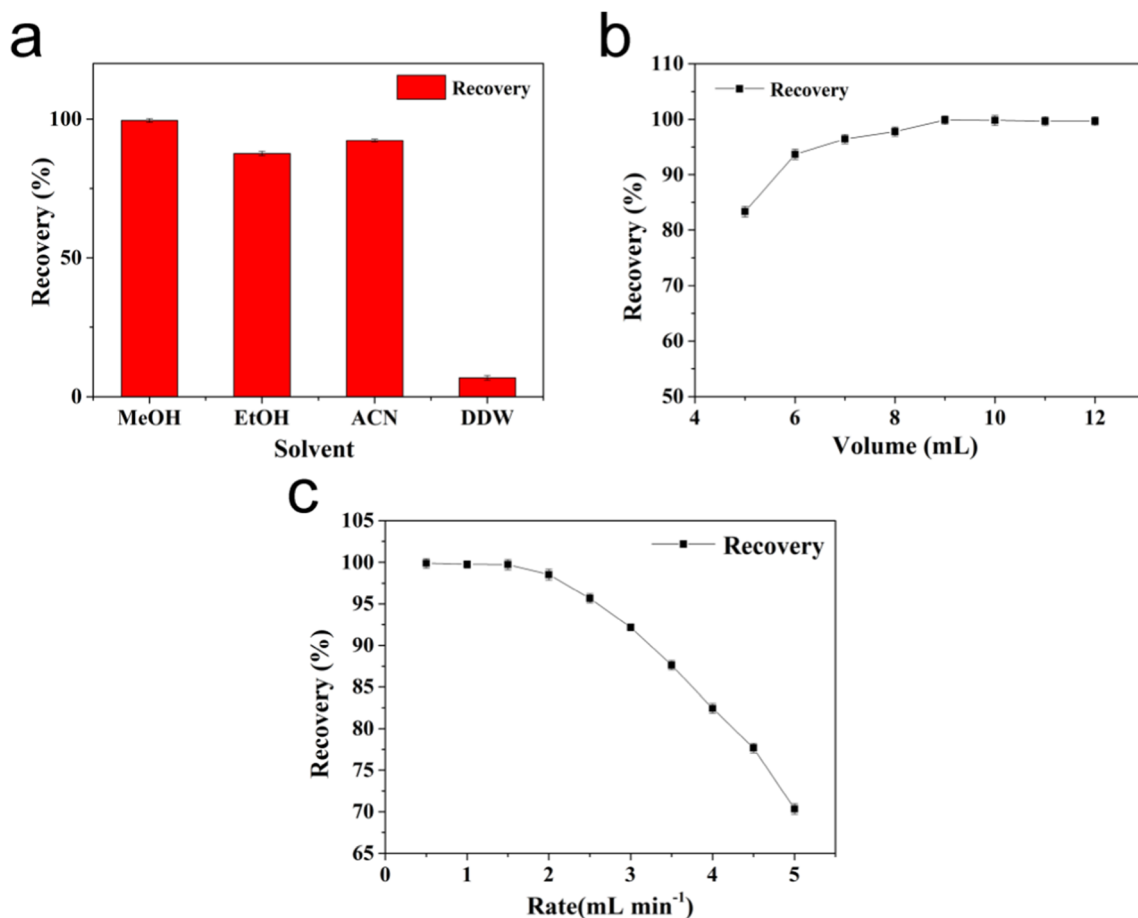
Fig. 6 The effects of different pH (**a**) and flow rate (**b**) on adsorption properties

Fig. 7 The effects of different solvent (**a**), volume (**b**), and rate (**c**) on adsorption properties

It was observed that the elution effect of MeOH was better in the four eluents under the same conditions. And 9 mL of MeOH could complete the elution and achieve 99.87% recovery. To ensure that the target was completely eluted and to avoid waste, 10 mL of MeOH was used in the experiment. At an elution flow rate of 0.5–1.5 mL min^{-1}, the recovery rate did not change significantly. Once the flow rate exceeded 1.5 mL min^{-1}, the recovery rate continued to decrease as the

flow rate increased. To achieve a better elution effect and improve the efficiency, an elution rate of 10 mL was selected.

Study on SPE Reusability and Comparison with Other Adsorption Materials

The MIP-SPE column, NIP-SPE column, and C18-SPE column were injected 50 mL of 1 mg L^{-1} carbaryl aqueous solution at a

Fig. 8 The SPE reusability (**a**), the recovery of different adsorption materials (**b**)
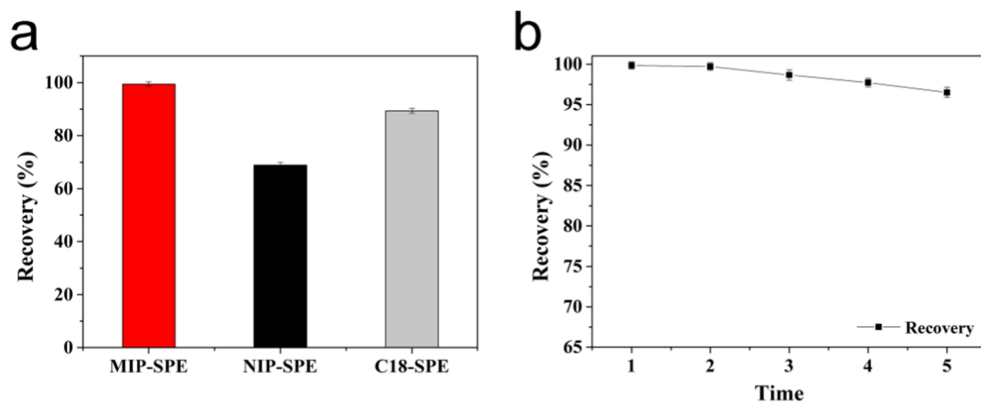
flow rate of 1 mL min^{-1} at a pH of 7–7.5 and eluted with 10 mL of MeOH at a flow rate of 1.5 mL min^{-1}; then, the recovery was calculated. It was can be seen in Fig. 8a that the recovery of the MIP-SPE column was far superior, which may be because the selectivity of MIP allowed it to capture the target more specifically to adsorb as much target as possible.

The MIP-SPE column was loaded with 50 mL of 1 mg L^{-1} carbaryl. The same column was reused 5 times and the recovery was measured to verify the recyclability of the SPE column. As shown in Fig. 8b, the recovery rates of the same MIP-SPE column changed smoothly with repeated use 5 times, and it could still reach 96.5% in the fifth use. Thus, this MIP-SPE column had good recyclability, which not only helped to save the MIP materials but also reflected the good adsorption performance of this MIP material.

The Characteristic Quantities of SPE-HPLC

Under the optimized experimental conditions, the standard curve of MIP-SPE-HPLC analysis was obtained. There was a good linear relationship ($R^2 = 0.99913$) and a low detection limit (0.0573 μg L^{-1}, RSD = 1.81%) was maintained in the concentration range of 5–60 μg L^{-1}.

Condition Optimization and Establishment of the MIP-QCM Detection Method

Optimization Experiment of the MIP-QCM Sensor

The different ratios of the mixture of PVC and MIP modified on the electrode by drop coating affect the frequency response of the sensor. Theoretically, while more PVC was beneficial to fix the MIP material on the electrode surface more stably, it may also reduce the sensitivity and specificity of the sensor because a high proportion of PVC is not conducive to the MIP binding site exposed to the solution, making it difficult for the target molecule to bind to the MIP specifically. Therefore, the maximum possible amount of MIP should be used to ensure high sensitivity while ensuring that the modification layer is

stable. The frequency shifts of the sensors modified with different proportions of PVC and MIP (PVC:MIP = 1:1, 1:2, 1:3, 1:4, 1:5, and 1:6, m:m) were determined in a 60 μg L^{-1} carbaryl standard solution and the results are shown in Fig. 9a. Keeping the quality of the PVC in the mixture unchanged and increasing the proportion of the MIP, the change value Δf of the response frequency of the sensor also increased. When PVC:MIP = 1:5 (m:m), the sensor frequency signal was reduced by 217 Hz, but it did not change much compared to the response frequency when PVC:MIP = 1:4 (m:m). If the amount of MIP was further increased, the Δf value showed a downward trend, which may be because the modified MIP was too much to firmly bond to the electrode. Therefore, considering the stability of the response frequency of the sensor, PVC:MIP = 1:4 was selected for the subsequent experiments.

In addition, different amounts of modification have a large impact on the sensitivity and stability of the sensor. In theory, increasing the thickness of the sensitive layer coating, that is, increasing the amount of MIP, can lead to the adsorption of more targets. However, the film that was too thick may fall off during the detection process, resulting in unstable frequency variation and causing the MIP particles to cover each other, affecting their binding to the target. Therefore, different amounts of DCM (5 μL, 10 μL, 15 μL, 20 μL, 25 μL, and 30 μL) containing MIP and PVC (4:1, m:m) were dropped on the surface of the electrode for experiments. As shown in Fig. 9b, as the modification amount of the sensitive material was increased, the frequency shifts of the sensor increased. When the amount added dropwise was in the range of 5 to 20 μL, the frequency increased greatly and then reached the maximum at 25 μL. However, during the experiment, it was found that the sensor signal stability decreased when the coating amount reached 25 μL and 30 μL. Therefore, 20 μL was chosen as the optimal amount of modification for the sensitive material.

Evaluation of Binding Performance

The response frequency changes of the established MIP-QCM sensor and NIP-QCM sensor were measured to evaluate their

Fig.9 a Effect of different ratio of MIP to PVC on the QCM sensor. b Effect of different modification amounts on the QCM sensor
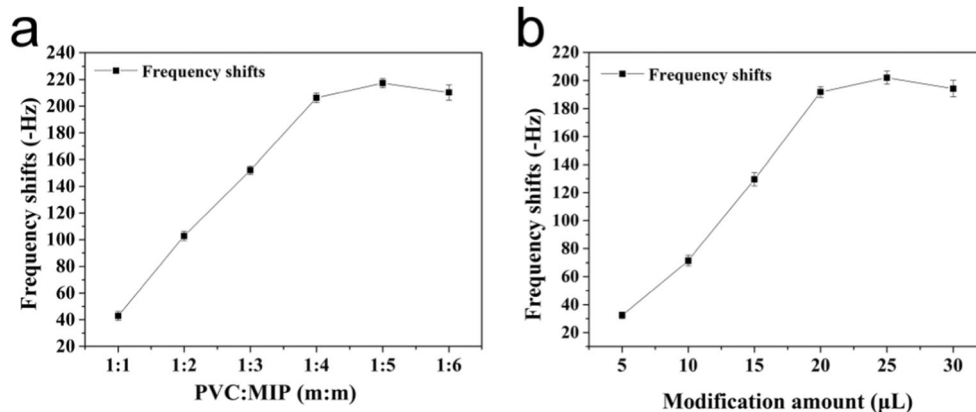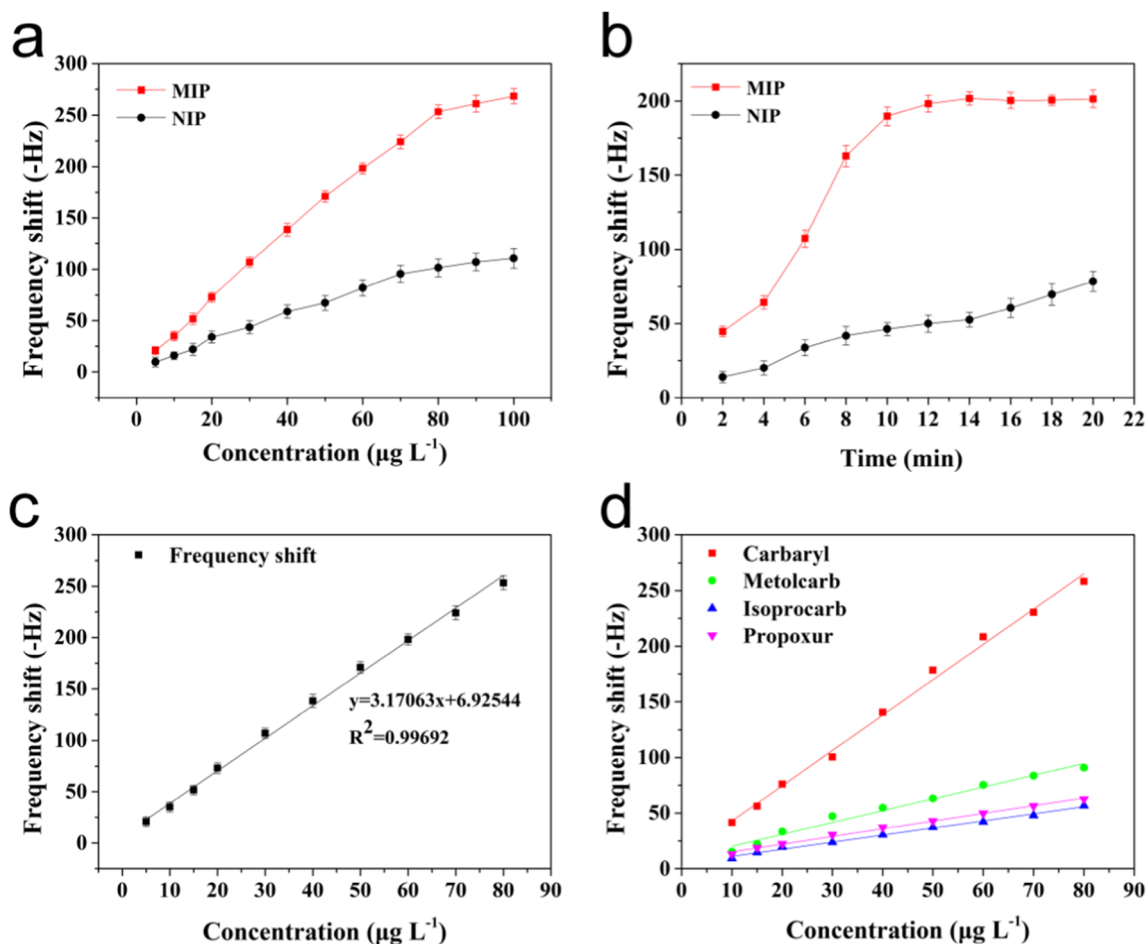
Fig.10 **a** Frequency shifts of MIP-QCM and NIP-QCM sensors towards different concentrations of carbaryl. **b** Adsorption equilibrium time curve of MIP-QCM and NIP-QCM sensors. **c** The standard curve of the MIP-QCM. **d** MIP-QCM sensor response to different analytes

Table 1 Recoveries of carbaryl from spiked samples determined by QCM sensor and HPLC

	Added (µg kg^{-1}/ µg L^{-1})	Purified with C18				Purified with MIP			
		HPLC		QCM		HPLC		QCM	
		Found (µg kg^{-1}/ µg L^{-1})	Recovery%(mean ± SD, $n=3$)	Found (µg kg^{-1}/ µg L^{-1})	Recover% (mean ± SD, $n=3$)	Found (µg kg^{-1}/ µg L^{-1})	Recovery% (mean ± SD, $n=3$)	Found (µg kg^{-1}/ µg L^{-1})	Recovery% (mean ± SD, $n=3$)
Apple juice	50	47.23 ± 1.7	94.5 ± 3.5	45.50 ± 1.8	91.0 ± 3.7	47.66 ± 1.5	95.3 ± 3.0	46.70 ± 1.1	93.5 ± 2.2
	100	93.73 ± 3.0	92.7 ± 3.0	91.73 ± 3.0	91.7 ± 3.0	94.58 ± 2.1	94.6 ± 2.1	93.43 ± 2.0	93.4 ± 2.0
	200	189.37 ± 2.6	94.7 ± 1.3	183.37 ± 2.6	91.7 ± 1.3	191.02 ± 2.9	95.5 ± 1.9	190.67 ± 1.9	95.3 ± 0.9
Pear	50	42.56 ± 2.4	85.1 ± 4.8	42.13 ± 2.4	84.3 ± 4.8	46.07 ± 2.6	92.1 ± 5.3	45.33 ± 2.6	90.7 ± 5.2
	100	85.26 ± 3.3	85.3 ± 3.3	87.76 ± 3.9	87.8 ± 3.9	89.08 ± 2.4	89.1 ± 2.4	87.56 ± 3.4	87.6 ± 3.4
	200	174.06 ± 4.3	87.0 ± 2.2	174.76 ± 4.1	87.4 ± 2.0	178.53 ± 3.3	89.3 ± 1.7	180.81 ± 3.7	90.4 ± 1.9
Round lettuce	50	43.20 ± 2.2	86.4 ± 4.5	42.70 ± 1.7	85.4 ± 3.5	45.53 ± 1.7	91.1 ± 3.5	44.90 ± 3.3	89.8 ± 6.5
	100	85.31 ± 1.9	85.31 ± 1.9	84.70 ± 2.4	84.7 ± 2.4	90.20 ± 3.1	90.2 ± 3.1	87.60 ± 2.6	87.6 ± 2.6
	200	173.53 ± 2.6	86.8 ± 1.3	174.33 ± 3.9	87.2 ± 2.0	181.73 ± 3.8	90.9 ± 1.9	177.43 ± 4.7	88.7 ± 2.4

Table 2 Comparison of analytical parameters for the determination of carbaryl

Analytical method	Sample	Linear range	Detection limit	Recovery (%)	Reference	Year
MIP-SPE-HPLC	apple juice, pear, round lettuce	0.5–60 µg L^{-1}	0.0573 µg L^{-1}	89.1–95.5	In this article	
MIP-QCM		5–80 µg L^{-1}	0.6845 µg L^{-1}	87.6–95.3		2018
Colorimetric	apple	50–500 µM (calibration curve range)	Below 10 ppm		Lee et al. (2018)	2018
CB-SPE	soft wheat, hard wheat and maize	1.0 × 10^{-7}–1.0 × 10^{-4} mol L^{-1}	≤ 8.0 × 10^{-8} mol L^{-1}	78–102	Pelle et al. (2018)	2018
SERS	fruit juices (orange and grapefruit), and milk	0–1000 ppb	50 ppb	82–97.5	Alsammarraie and Lin (2017)	2017
Electrochemistry	tomatoes, apples, peaches, cucumbers, and grapes; vegetables; and water	0.004–0.3 µM	0.0012 µM	96.2–104.0	Rahmani et al. (2018)	2018
BELISA	rice, Chinese cabbage	0.001–1 mg L^{-1}	0.007 mg L^{-1}	79.7–103.8	Zhang et al. (2017)	2017
HFF-QCM immunosensor		0.26–1.73 µg L^{-1} (working range)	0.14 µg L^{-1}		Bruckenstein and Shay (1985)	2015
HFF-QCM	honey	0.195–1.108 µg L^{-1} in PBS, 0.083–1.572 µg L^{-1} in 1/200 diluted honey (working range)	0.118 µg L^{-1} in PBS, 0.035 µg L^{-1} in 1/200 diluted honey	110–117	Carmen (2015)	2018

binding properties in the carbaryl concentration range of 10.0–100.0 µg L^{-1} at room temperature. Figure 10a shows that the frequency shift of the MIP-QCM and NIP-QCM sensors increased with increasing carbaryl concentration. MIP-QCM always achieved a greater frequency shift at any concentration within the experimental concentration range, which indicated that the MIP-QCM sensor had a stronger binding ability to the target.

The static adsorption experiment was carried out under a carbaryl concentration of 60 µg L^{-1} and the results are shown in Fig. 10b. The MIP-QCM can reach adsorption equilibrium faster, and adsorption can be completed in 12–14 min, which can be attributed to the larger specific surface area of the MIP.

In 100 µg L^{-1} carbaryl, the frequency shift of the MIP sensor was − 268.5 Hz while that of the NIP sensor was − 110.8 Hz. The MIP sensor had a distinct advantage over the NIP sensor, owing to the imprinted cavity formed during the material synthesis process. As shown in Fig. 10c, a linear correlation was observed between the frequency shifts and the concentrations of carbaryl ranging from 5 to 80 µg L^{-1} with an R^2 value of 0.9945. The detection limit (S/N = 3) reached 0.6845 µg L^{-1}. In addition, the PVC-coated electrode as a control did not generate a frequency shift, which indicated that PVC did not adsorb the target and did not contribute to the experimental results.

It was important that the proposed MIP-QCM sensor could selectively identify and adsorb the target in a complicated food matrix in practical applications. Three carbamate pesticides (metolcarb, isoprocarb, and propoxur) with similar structures were used to detect and evaluate the sensor's selective recognition ability. Figure 10d shows that the frequency shifts of the sensor in response to the target and the analytes were quite different. The SC (selectivity coefficient, SC analyte = $\alpha_{\text{carbaryl}}/\alpha_{\text{analyte}}$, where α is the slope of the analyte calibration curve) was used to quantify the selective adsorption ability of the sensor to these analytes. The SC values of carbaryl towards metolcarb, isoprocarb, and propoxur were calculated to be 2.994, 5.29, and 4.6, respectively, showing the excellent selective adsorption capacity of the prepared MIP-QCM sensor.

Moreover, the ratio of the frequency shift ($\Delta f_m/\Delta f_0$, where f_m and f_0 are the frequency shifts towards carbaryl with and without interferences) was calculated to evaluate the anti-interference capability of the prepared MIP-QCM sensor. When the same concentration of interferents existed, $\Delta f_m/\Delta f_0$ slightly varied from 99.87 to 107.34%. These data demonstrated that the established sensor detection method had preeminent stability and was resistant to interference from structural analogues.

Furthermore, the reproducibility of the prepared MIP-QCM sensor was assessed by duplicate testing

of the frequency shifts in the 60 µg L^{-1} carbaryl standard solution 6 times reusing the same MIP electrode. Before each new measurement, the electrode was washed with the configured eluant (MeOH: 1 mol L^{-1} hydrochloric acid, 9:1, v/v) and DDW alternately until the frequency reached its initial value. The obtained value was used to calculate the relative standard deviation (RSD). The RSD = 1.447%, indicating that the prepared MIP-QCM sensor had excellent reusability.

Real Sample Analysis

To further verify the practical viability of the prepared MIP-QCM sensor, spiking and recovery studies were carried out, which analysed trace carbaryl in apple juice, pear, and round lettuce. The statistical results are shown in Table 1. After purification with a C18 column, decent recoveries ranging from 84.3 to 91.7% with an RSD ($n = 3$) of 1.4–5.7% were obtained. The results were consistent with the results (mean recoveries, 85.3–94.7%) determined by HPLC. At the same time, the corresponding recovery ranges obtained by purification with the MIP-SPE column were 87.6–95.3% (QCM, RSD 1.0–6.9%) and 90.2–95.5% (HPLC, RSD 1.8–5.6%). It was confirmed that the MIP material synthesized by this method had good specific adsorption capacity, and the proposed MIP-QCM sensor was reliable and effective for analysing trace carbaryl in practical samples.

Brief Comparison with Other Methods

Compared with other detection methods, the method established in this paper has different advantages in terms of detection range and detection limit (Table 2). Compared with colorimetric, CB-SPE, SERS, and BELISA methods, the methods established in this work had a narrow linear detection range but a lower detection limit in the trace detection of pesticide residues. The detection limits of the HFF-QCM immunoassay and HFF-QCM were lower, but the linear range was excessively narrow. The detection limit and linear range of the method established in this work were relatively close to those of the electrochemical method, but the preparation of the proposed methods was more economical and easy to popularize. The advantages of simple operation and strong reusability make this approach widely applicable in practical detection.

Conclusions

In this study, MIP materials with specific adsorption to carbaryl were synthesized on the basis of grafted modified silicon spheres. Then, the MIP was separately applied to SPE-HPLC

and QCM sensors, and the two detection methods were used to detect carbaryl in food samples. The results show that the MIP material has a large adsorption capacity and accurate recognition ability, so it can accurately and specifically capture the target as the material for solid-phase extraction and can sensitively and quickly determine the carbaryl as the coating on the QCM sensor. This work also provides a promising approach for imprinting, selective separation, and rapid detection of other carbamate pesticides from complicated matrices.

Compliance with Ethical Standards

Conflict of Interest Chang Liu declares that he/she has no conflict of interest. Yichuan Cao declares that he/she has no conflict of interest. Tian Zhao declares that he/she has no conflict of interest. Xiaohui Wang declares that he/she has no conflict of interest. Guozhen Fang declares that he/she has no conflict of interest. Shuo Wang has no conflict of interest.

Research Involving Human Participants and/or Animals Not applicable. This study does not involve human participants and/or animals.

Informed Consent Informed consent not applicable.

References

Alsammarraie FK, Lin M (2017) Using standing gold nanorod arrays as surface-enhanced Raman spectroscopy (SERS) substrates for detection of carbaryl residues in fruit juice and milk. Journal of Agricultural & Food Chemistry 65:666–674. https://doi.org/10.1021/acs.jafc.6b04774

Ayankojo AG, Reut J, Boroznjak R, Öpik A, Syritski V (2018) Molecularly imprinted poly(meta-phenylenediamine) based QCM sensor for detecting amoxicillin sensors and actuators B: Chemical 258:766-774 doi:https://doi.org/10.1016/j.snb.2017.11.194

Bruckenstein S, Shay M (1985) Experimental aspects of use of the quartz crystal microbalance in solution Electrochimica Acta 30:1295–1300 doi:https://doi.org/10.1016/0013-4686(85)85005-2

Carmen et al (2015) High-frequency phase shift measurement greatly enhances the sensitivity of QCM immunosensors Biosensors & Bioelectronics. 65:1–8. https://doi.org/10.1016/j.bios.2014.10.001

Cervera-Chiner L, Juan-Borrás M, March C, Arnau A, Jiménez Y (2018) High Fundamental Frequency Quartz Crystal Microbalance (HFF-QCM) immunosensor for pesticide detection in honey Food Control 92:1–6 doi:https://doi.org/10.1016/j.foodcont.2020.107296

European Commission (2014) Commission Regulation (EU) No 1096/2014 of 15 October 2014 https://ec.europa.eu/food/plant/pesticides/eu-pesticides-database/public/?event=pesticide.residue.selection&language=EN

Gaudin V (2017) Advances in biosensor development for the screening of antibiotic residues in food products of animal origin – a comprehensive review Biosensors & Bioelectronics 90:363-377 doi:https://doi.org/10.1016/j.bios.2016.12.005

GB2763-2019, China (2019) National food safety standard-maximum residue limits for pesticides in food China:131

Gültekin A, Karanfil G, Kuş M, Sönmezoğlu S, Say R (2014) Preparation of MIP-based QCM nanosensor for detection of caffeic acid Talanta 119:533–537 doi:https://doi.org/10.1016/j.talanta.2013.11.053

Gültekin A, Karanfil G, Sonmezoglu S, Say R (2014) Development of a highly sensitive MIP based-QCM nanosensor for selective determination of cholic acid level in body fluids Mater Sci Eng C Mater Biol Appl 42:436–442. https://doi.org/10.1016/j.msec.2014.05.055

Hargreaves PA, Melksham KJ (1983) A rapid high-pressure liquid chromatographic method for the determination of carbaryl residues in wheat grain Pesticide Science 14:347–353 doi:https://doi.org/10.1002/ps.2780140402

Hernández F, Cervera MI, Portolés T, Beltrán J, Pitarch E (2013) The role of GC-MS/MS with triple quadrupole in pesticide residue analysis in food and the environment Analytical Methods 5:5875–5894 doi:https://doi.org/10.1039/c3ay41104d

Husseman M et al. (1999) Controlled synthesis of polymer brushes by "living" free radical polymerization techniques macromolecules 32:1424-1431 doi:https://doi.org/10.1021/ma981290v

Karami-Mohajeri S, Abdollahi M (2011) Toxic influence of organophosphate, carbamate, and organochlorine pesticides on cellular metabolism of lipids, proteins, and carbohydrates: a systematic review. Human & Experimental Toxicology 30:1119–1140. https://doi.org/10.1177/0960327110388959

Karousos NG, Aouabdi S, Way AS, Reddy SM (2002) Quartz crystal microbalance determination of organophosphorus and carbamate pesticides Analytica Chimica Acta 469:189–196 doi:https://doi.org/10.1016/S0003-2670(02)00668-2

Lee MG, Patil V, Na YC, Lee DS, Lim SH, Yi GR (2018) Highly stable, rapid colorimetric detection of carbaryl pesticides by azo coupling reaction with chemical pre-treatment. Sensors & Actuators B Chemical 261:489–496. https://doi.org/10.1016/j.snb.2018.01.151

Lin T, Hu C, Tc (2005) Determination of albumin concentration by MIP-QCM sensor Biosensors & Bioelectronics 20:75–81 doi:https://doi.org/10.1016/j.bios.2004.01.028

Pelle FD, Angelini C, Sergi M, Carlo MD, Pepe A, Compagnone D (2018) Nano carbon black-based screen printed sensor for carbofuran, isoprocarb, carbaryl and fenobucarb detection: application to grain samples. Talanta 186:389–396. https://doi.org/10.1016/j.talanta.2018.04.082

Petropoulou SSE, Anthony T, Siskos PA (2006) Determination of carbofuran, carbaryl and their main metabolites in plasma samples of agricultural populations using gas chromatography-tandem mass spectrometry. Analytical & Bioanalytical Chemistry 385:1444–1456. https://doi.org/10.1007/s00216-006-0569-0

Rahmani T, Bagheri H, Behbahani M, Hajian A, Afkhami A (2018) Modified 3D graphene-Au as a novel sensing layer for direct and sensitive electrochemical determination of carbaryl pesticide in fruit, vegetable, and water samples. Food Analytical Methods 11:3005–3014. https://doi.org/10.1007/s12161-018-1280-4

Spieker E, Lieberzeit PA (2016) Molecular imprinting studies for developing QCM-sensors for Bacillus cereus. Procedia Engineering 168:561–564. https://doi.org/10.1016/j.proeng.2016.11.525

Sun J, Dong T, Zhang Y, Wang S (2010) Development of enzyme linked immunoassay for the simultaneous detection of carbaryl and metolcarb in different agricultural products Analytica Chimica Acta 666:76–82 doi:https://doi.org/10.1016/j.aca.2010.03.051

The Japan Food Chemical Research Foundation (2019) Addition of an agricultural chemical, revision of MRLs of agricultural chemicals, and veterinary drugs in foods http://db.ffcr.or.jp/front/pesticide_detail?id=16400

U.S. GPO (2020) Tolerances and exemptions for pesticide chemical residues in food. https://www.ecfr.gov/cgi-bin/text-idx?SID=2c85909360c7c5aff63ddd1447545d6a&mc=true&node=se40.24.180_1169&rgn=div8

Zhang C, Cui H, Han Y, Yu F, Shi X (2017) Development of a biomimetic enzyme-linked immunosorbent assay based on molecularly imprinted polymers on paper for the detection of carbaryl. Food Chemistry 240:893–897. https://doi.org/10.1016/j.foodchem.2017.07.109